A photonic spectral processor employing two-dimensional WDM channel separation and a phase LCoS modulator

David Sinefeld,[1,*] Christopher R. Doerr,[2] and Dan M. Marom[1]

[1] *Applied Physics Department, Hebrew University, Jerusalem 91904, Israel*
[2] *Bell Laboratories, Alcatel-Lucent, 791 Holmdel-Keyport Rd., Holmdel, NJ 07733, USA*
[*] *sinefeld@gmail.com*

Abstract: We present a Photonic Spectral Processor (PSP) that provides both fine spectral resolution and broad bandwidth support by dispersing light over two-dimensional space using the crossed-grating approach. The PSP uses a hybrid guided wave/free-space optics arrangement, where a waveguide grating router implemented in silica waveguides disperses the light in one dimension with a 100 GHz FSR and a bulk 1200 gr/mm diffraction grating disperses the light along the second (crossed) dimension. The diffracted light is focused by a lens onto a liquid-crystal on silicon, two-dimensional, phase-only, spatial light modulator, which we use to prescribe phase and amplitude to the signal's spectral components. With the 2-D PSP arrangement we are able to address frequency components at 0.2 GHz/column with an optical resolution of 3.3 GHz covering 40 C-band channels.

OCIS codes: (060.2330) Fiber optics communications; (130.2035) Dispersion compensation devices; (130.7408) Wavelength filtering devices.

References and links

1. M. A. F. Roelens, S. Frisken, J. A. Bolger, D. Abakoumov, G. Baxter, S. Poole, and B. J. Eggleton, "Dispersion trimming in a reconfigurable wavelength selective switch," J. Lightwave Technol. **26**(1), 73–78 (2008).
2. D. T. Neilson, R. Ryf, F. Pardo, V. A. Aksyuk, M. E. Simon, D. O. Lopez, D. M. Marom, and S. Chandrasekhar, "MEMS-based channelized dispersion compensator with flat passbands," J. Lightwave Technol. **22**(1), 101–105 (2004).
3. D. T. Neilson, H. Tang, D. S. Greywall, N. R. Basavanhally, L. Ko, D. A. Ramsey, J. D. Weld, Y. L. Low, F. Pardo, D. O. Lopez, P. Busch, J. Prybyla, M. Haueis, C. S. Pai, R. Scotti, and R. Ryf, "Channel equalization and blocking filter utilizing microelectromechanical mirrors," IEEE J. Sel. Top. Quantum Electron. **10**(3), 563–569 (2004).
4. S. Sohma, K. Mori, H. Masuda, A. Takada, K. Seno, K. Suzuki, and N. Ooba, "Flexible chromatic dispersion compensation over entire L-band for over 40-Gb/s WDM transparent networks using multichannel tunable optical dispersion compensator," IEEE Photon. Technol. Lett. **21**(17), 1271–1273 (2009).
5. M. Shirasaki, "Chromatic dispersion compensator using virtually imaged phased array," IEEE Photon. Technol. Lett. **9**(12), 1598–1600 (1997).
6. C. R. Doerr, R. Blum, L. L. Buhl, M. A. Cappuzzo, E. Y. Chen, A. Wong-Foy, L. T. Gomez, and H. Bulthuis, "Colorless tunable optical dispersion compensator based on a silica arrayed-waveguide grating and a polymer thermooptic lens," IEEE Photon. Technol. Lett. **18**(11), 1222–1224 (2006).
7. D. M. Marom, C. R. Doerr, M. A. Cappuzzo, E. Y. Chen, A. Wong-Foy, L. T. Gomez, and S. Chandrasekhar, "Compact colorless tunable dispersion compensator with 1000-ps/nm tuning range for 40-Gb/s data rates," J. Lightwave Technol. **24**(1), 237–241 (2006).
8. D. Sinefeld and D. M. Marom, "Colorless photonic spectral processor using hybrid guided-wave/free-space optics arrangement and LCoS modulator," in *Proceedings of Optical Fiber Communication Conference and Exposition* (Optical Society of America, 2009), paper OThB4.
9. D. Sinefeld and D. M. Marom, "Hybrid guided-wave/free-space optics photonic spectral processor based on LCoS phase only modulator," IEEE Photon. Technol. Lett. **22**(7), 510–512 (2010).
10. K. Suzuki, N. Ooba, M. Ishii, K. Seno, T. Shibata, and S. Mino, "40-wavelength channelized tunable optical dispersion compensator with increased bandwidth consisting of arrayed waveguide gratings and liquid crystal on silicon," in *Proceedings of Optical Fiber Communication Conference and Exposition* (Optical Society of America, 2009), paper OThB3.

#149409 - $15.00 USD Received 16 Jun 2011; revised 30 Jun 2011; accepted 30 Jun 2011; published 13 Jul 2011

11. K. Seno, N. Ooba, K. Suzuki, T. Watanabe, K. Watanabe, and S. Mino, "Tunable optical dispersion compensator consisting of simple optics with arrayed waveguide grating and flat mirror," IEEE Photon. Technol. Lett. **21**(22), 1701–1703 (2009).
12. D. Sinefeld, S. Ben-Ezra, C. R. Doerr, and D. M. Marom, "All-channel tunable optical dispersion compensator based on linear translation of a waveguide grating router," Opt. Lett. **36**(8), 1410–1412 (2011).
13. D. Sinefeld and D. M. Marom, "Spectral processor implemented with hybrid free-space and guided-wave optics and active LCoS modulator," in *Proceedings of IEEE 25th Convention of Electrical and Electronics Engineers in Israel*, 380–383 (2008).
14. K. Seno, K. Suzuki, N. Ooba, K. Watanabe, M. Ishii, H. Ono, and S. Mino, "Demonstration of channelized tunable optical dispersion compensator based on arrayed-waveguide grating and liquid crystal on silicon," Opt. Express **18**(18), 18565–18579 (2010).
15. T. K. Chan, J. Karp, R. Jiang, N. Alic, S. Radic, C. F. Marki, and J. E. Ford, "1092 channel 2-D array demultiplexer for ultralarge data bandwidth," J. Lightwave Technol. **25**(3), 719–725 (2007).
16. V. R. Supradeepa, C. B. Huang, D. E. Leaird, and A. M. Weiner, "Femtosecond pulse shaping in two dimensions: towards higher complexity optical waveforms," Opt. Express **16**(16), 11878–11887 (2008).
17. D. Sinefeld, C. R. Doerr, and D. M. Marom, "Photonic spectral processor employing two-dimensional WDM channel separation and a phase LCoS modulator," in *Proceedings of Optical Fiber Communication Conference and Exposition* (Optical Society of America, 2010), paper OMP5.
18. K. Seno, K. Suzuki, N. Ooba, T. Watanabe, M. Itoh, S. Mino, and T. Sakamoto, "50-wavelength channel-by-channel tunable optical dispersion compensator using combination of arrayed-waveguide and bulk gratings," in *Optical Fiber Communication Conference and Exposition*, (Optical Society of America, 2010), paper OMT7.
19. K. Seno, K. Suzuki, N. Ooba, T. Watanabe, M. Itoh, S. Mino, and T. Sakamoto, "50-wavelength channel-by-channel tunable optical dispersion compensator using a combination of AWG and bulk grating," IEEE Photon. Technol. Lett. **22**(22), 1659–1661 (2010).
20. C. K. Madsen and J. H. Zhao, *Optical filter design and analysis: A signal processing approach* (Wiley-Interscience, 1999).
21. J. Leuthold, D. Marom, S. Cabot, J. Jaques, R. Ryf, and C. Giles, "All-optical wavelength conversion using a pulse reformatting optical filter," J. Lightwave Technol. **22**(1), 186–192 (2004).
22. S. Sygletos, R. Bonk, T. Vallaitis, A. Marculescu, P. Vorreau, J. Li, R. Brenot, F. Lelarge, G.-H. Duan, W. Freude, and J. Leuthold, "Filter assisted wavelength conversion with quantum-dot SOAs," J. Lightwave Technol. **28**(6), 882–897 (2010).
23. H. Schenk, H. Gruger, F. Zimmer, W. Scherf, and A. Kenda, "Optical MEMS for advanced spectrometers," in *Proceedings of IEEE/LEOS Conf. on Optical MEMS*, 117–118 (2005).

1. Introduction

Optical devices independently controlling the transmission of individual channels are important for maximizing the performance of WDM optical communication systems. Channel power equalizers are required for maintaining the same OSNR across all amplified channels in a long-haul system. Dispersion compensators are essential in communication systems employing direct or differential detection, and can reduce the processing overhead in coherent reception systems. With increasing channel transmission rates, the broad signal spectrum becomes more susceptible to filtering and dispersion, resulting in a degraded signal reaching the receiver. One promising class of impairment mitigation devices uses spatial dispersion to separate the light's frequency components together with a spatial light modulator (SLM) in applying an adaptive filtering function [1–5]. The optical performance of these spectral processing devices depends on the spectral resolution and spectral addressability, which are a function of the dispersing optics solution and the SLM technology. Colorless devices use an engineered dispersing element with a free-spectral range (FSR) matching the channel plan [6–12], imparting identical functionality to every channel but with very high resolution. Broadband devices use dispersing elements with a FSR matching or exceeding the whole communication band, which limits the optical resolution of the system [13-14]. These devices demonstrate that the optical dispersion arrangements provide a finite space-bandwidth product that can be allocated to either broad bandwidth at coarse resolution or narrow bandwidth at fine resolution. This space-bandwidth limitation can be overcome by dispersing over two-dimensional space, capitalizing on the additional transverse spatial dimension available with free-space optics. The typical crossed-dispersion optics solution utilizes two gratings where the first has a small FSR with fine resolving capability, and the second crossed grating has a large FSR that separates the diffraction orders of the first grating. This kind of arrangement was introduced before as a solution for a high resolution demultiplexer [15] as well as for pulse shaping [16].

#149409 - $15.00 USD Received 16 Jun 2011; revised 30 Jun 2011; accepted 30 Jun 2011; published 13 Jul 2011

Last year, we presented a two-dimensional, amplitude and phase, photonic spectral processor (PSP) with the ability to control each WDM channel in separately [17], and had the same high resolution as our earlier colorless PSP [9]. This PSP was based on the combination of two crossed gratings, a high resolution waveguide grating router (WGR) and a free-space bulk grating, together with a liquid crystal on silicon (LCoS), two-dimensional, pixelated phase modulator. An identical arrangement was simultaneously inroduced by Seno at al [18, 19], but their work demonstrated only tunable dispersion compensation. In this work we discuss the full design consideration of such a two dimensional system, with the addition of new and improved results over those reported in [17], demonstrating the ability to manipulate both spectral phase and amplitude along the conventional optical communication band (1530-1560 nm), with a resolution of 3.3 GHz and 0.2 GHz addressability.

2. System design considerations

Our PSP is based on a hybrid guided wave / free-space optics arrangement, where a WGR implemented in silica waveguides disperses the light in one dimension with a 100 GHz FSR and a bulk 1200 gr/mm diffraction grating disperses the light along the second (crossed) dimension and separates the diffraction orders of the WGR grating. The diffracted light is then focused by a Fourier lens onto an LCoS, two-dimensional phase SLM. With the LCoS SLM we are able to prescribe phase and amplitude to the signal's spectral components.

The PSP layout and concept is depicted in Fig. 1. Light enters a planar lightwave circuit (PLC) containing an extremely high resolution WGR through the input/output (I/O) waveguide. The WGR was fabricated in silica-on-silicon technology with 0.8% index contrast waveguides and consists of 34 grating arms that are "pinched" in the middle for conserving wafer area, reducing the grating sensitivity to wafer refractive index gradients, and enables the insertion of a half-wave plate to make the WGR polarization-independent (not performed in this case as both the LCoS and bulk grating are polarization dependent). The output of the WGR is unconventional: instead of employing a second slab-lens region that demultiplexes to output waveguides, the grating arms terminate at the PLC edge and the light radiates to free-space. An f = 3mm cylindrical lens that is affixed at the PLC edge collimates the light in the guided direction.

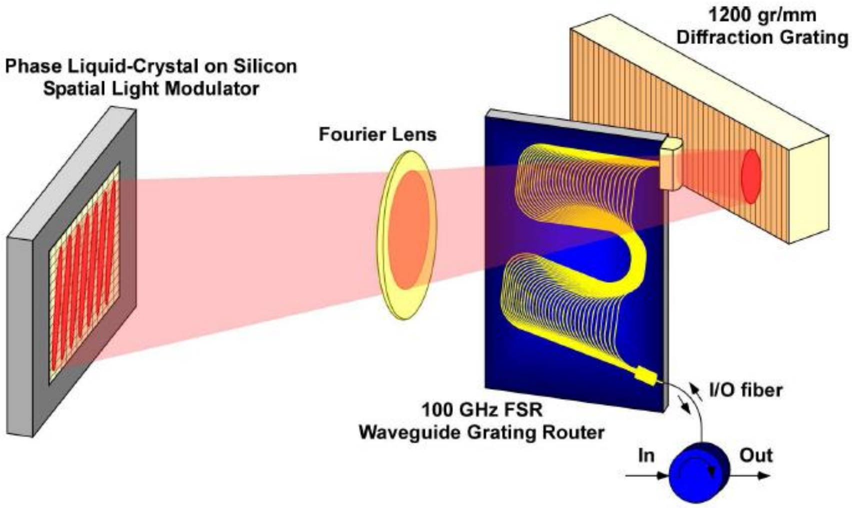

Fig. 1. Layout of the two-dimensional photonic spectral processor, capable of imparting independent spectral amplitude and phase to each WDM channel with the use of a LCoS modulator array. Crossed gratings (WGR and bulk) disperse the spectrum across the two-dimensional LCoS array, enabling high resolution access to the spectral components of each channel.

In a simple, colorless system [9], a Fourier lens is placed after the WGR output to observe the spatially-dispersed spectra at the lens back focal plane. In that case, the dispersed spectrum of all the WDM channels overlap onto each other, due to the WGR's 100 GHz FSR, and would be the basis for a colorless device. In our current 2D processor we place a crossed bulk grating between the WGR and the lens, separating the diffraction orders of the WGR in the orthogonal direction. This arrangement results in two spatial dispersion axes: a "fast" dispersion axis which has high resolution and 100 GHz FSR, and an orthogonal "slow" dispersion axis which separates the WDM channels. The diffraction spread angle of the beam in the "slow" axis is determined by the collimated size of the beam output after the cylindrical lens, according to:

$$\Delta\theta_{spot} = \frac{2\lambda}{\pi w_0} = \frac{2\lambda}{\pi f_{cyl} N.A._{WG}} \tag{1}$$

where $2w_0$ is the collimated size of the beam output, $\lambda = 1.55\mu\text{m}$ is the center wavelength, $f_{cyl} = 3\ mm$ is the cylindrical lens focal length, and $N.A._{WG} = 0.12$ is the waveguide output numerical aperture. To achieve WGR order separation we must use a bulk grating with an angular dispersion $(d\theta/d\nu)_{BG}$ greater than the diffraction spread angle:

$$\Delta\nu_{FSR} \cdot \left(\frac{d\theta}{d\nu}\right)_{BG} \geq \Delta\theta_{spot} \tag{2}$$

Using $\Delta\theta_{spot}$ from Eq. (1), and $\Delta\nu_{FSR} = 100\ GHz$ of the WGR, we can calculate the required dispersion in the "slow" dispersion axis. We utilize near Littrow mounting for our bulk grating. In this case the angular dispersion is determined by:

$$\left|\left(\frac{d\theta}{d\nu}\right)_{BG}\right| = \frac{\lambda^2}{c}\left(\frac{d\theta}{d\lambda}\right)_{BG} = \frac{\lambda^2}{c \cdot d\cos(\theta)} \tag{3}$$

where d is the grating period, λ is the wavelength, c is the speed of light and θ is the incidence/diffraction angle of the bulk grating. Combining Eqs. (1)–(3) results in the condition:

$$d\cos(\theta) \leq \frac{\pi\lambda f_{cyl} N.A._{WG} \Delta\nu_{FSR}}{2c} \tag{4}$$

We satisfy the condition set forth by Eq. (4) using a 1200 gr/mm holographic diffraction grating which was placed at an angle of approximately 73° (close to the 68.5° Littrow angle of such grating) in order to achieve the order separation for our 2D system. An IR-optimized $f = 100$mm cemented doublet lens performs the Fourier transform and converts the angular spectrum to spatial and projects 2D separated frequency components onto the LCoS SLM. We used a phase-only, two-dimensional LCoS reflective modulator manufactured by Boulder Nonlinear Systems and placed it at the spectral plane. The LCoS modulator has 512 × 512 square pixels of 15 μm pitch, providing an active region of 7.68 × 7.68 mm.

Ideally, both gratings should be placed at the lens front focal plane so that their angular dispersion will be converted to spatial dispersion that is normally-incident onto the SLM. This could be achieved with a multi-lens solution that images the first grating onto the second [16], but such a solution increases the optical track length and component count and is hence undesirable. Instead, we place the bulk grating in between the WGR (which is placed near the front focal plane) and the lens. This results in the grating orders being incident in a space-varying incidence angle, or curvature. This phase curvature is related to the distance of the grating from the first Fourier plane, Δz, according to the expression [12]:

$$\frac{1}{R} = \frac{\Delta z}{f^2} \tag{5}$$

#149409 - $15.00 USD Received 16 Jun 2011; revised 30 Jun 2011; accepted 30 Jun 2011; published 13 Jul 2011

where f is the focal length of the Fourier lens, and R is the phase radii. This unwanted curved phase will result in losses for off-axis channels. However, this effect can be completely compensated in our system since our phase LCoS SLM can encode a cylindrical quadratic phase function across the aperture. In this way we can couple-back the light from all diffraction orders with constant efficiency as shown in Fig. 2. Note that it is advantageous to displace the bulk grating from the front focal plane and not the WGR output, as the "fast" dispersion axis is more susceptible to chromatic dispersion being added onto the signal for an identical displacement [12].

3. System characteristics and basic performance

The elements of the two-dimensional PSP, consisting of the WGR PLC, bulk grating, lens, and the LCoS modulator were assembled on an optical table as shown in Fig. 1. A curved phase along the SLM slow-axis direction equalized the insertion loss along the different channels as discussed previously (see Fig. 2).

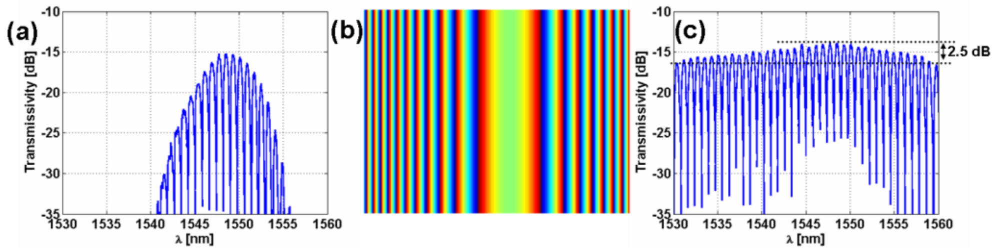

Fig. 2. The impact of applying horizontal curved phase along the channels in order to eliminate the losses caused by the finite separation between the WGR output facet and the bulk grating. (a) PSP output before equalization. (b) The horizontal quadratic phase that was added in order to achieve channel equalization. (c) PSP after equalization. In the plot 40 WDM channels are shown. This was achieved by moving the SLM along the spectral plane, and stitching the overlapping results from two SLM locations.

An intensity uniformity of 2.5 dB is achieved along 30 nm, resulting in 40 nearly equalized WDM channels. We should note that since our SLM is not physically large enough to span the entire c-band (it is sufficient for only 30 WDM channels), we had to transversely reposition the SLM and stitch together two spectra in order to record all the 40 channels as shown in Fig. 2. This result was measured without any other change in the optical setup, which means it could be easily achieved with a larger SLM. An alternative solution is to use a shorter focal length Fourier lens, but there was insufficient clearance for such an approach with a reflection grating.

To characterize the spatial dispersion, beam size and resolution of the PSP, a narrow line laser was tuned across the c-band, and its transmitted power through the system was recorded. For every wavelength, a 0-π vertical phase step transition pattern was applied, the location of this phase jump being scanned along the rows of the SLM (Fig. 3(b)). A similar horizontal phase step pattern was subsequently scanned along the columns of the SLM (Fig. 3(e)). Both step phase patterns were applied on top the base curved phase (Fig. 3(c) and 3(f)), which is always required for channel equalization. When the phase step occurs at the center of the laser line spot (in either horizontal or vertical direction), destructive interference between the two equal halves of the beam results in minimal output power coupling, thus identifying the beam position for every wavelength. Similarly, the onset and ending of the output power fluctuation measure the beam extent in the horizontal and vertical axes directions (as shown in Fig. 3(a), and 3(d)).

The spatial dispersion mapping is identified by locating the center position for each laser wavelength. In the WGR direction (fast axis) the SLM 512 columns spans a ~93-GHz wide spectrum (limited by SLM size) which correspond to spatial dispersion of 10.3[*mm/nm*]. Each column of the modulator addresses a particular center frequency, at 182 MHz shift in center frequency. The spatial dispersion in the bulk grating direction results in an offset of 15 pixels for successive diffraction orders (spaced at 100 GHz). This pitch is not constant across the

#149409 - $15.00 USD Received 16 Jun 2011; revised 30 Jun 2011; accepted 30 Jun 2011; published 13 Jul 2011

spectrum, as the grating angular dispersion is not linear. Figure 3(g) shows a mapping of the incident wavelengths onto the LCoS array. There is a slight deviation from linear dispersion on account of the bulk grating being offset from the lens focal plane. Due to the limited size of our LCoS SLM, only 30 WDM channels spaced at 100GHz can be modulated and reflected back at a time.

Using the same method, we measured the vertical and horizontal size of a single laser spot on the SLM. The vertical beam width was 18 pixels along the WGR (fast) dispersion direction at −3 dB. This determines the resolution of the system which equals *18 x 0.182 = 3.3 GHz*. One should note the distinction between spectral resolution and addressability: the resolution defines the smallest feature that can be controlled with the system, while the addressability defines the amount of minimal change in the center wavelength of any spectral feature controlled with the PSP. Scanning the SLM in the bulk (slow) direction gave a beam width of 15 pixels (full width measured at 0 dB level in the horizontal direction as shown in Fig. 3(d)), which is exactly the separation between diffraction orders along the SLM. This result demonstrates that each diffraction order is just barely resolved in our implementation.

After defining the spatial dispersion mapping, we can assign spectral modulation to the dispersed components (subject to resolution limitations). Phase modulation to a spectral component is achieved by prescribing an identical phase to all pixels within the beam corresponding to the spectral component (18 pixels height) in the WGR direction. Amplitude modulation is achieved by setting a linear phase ramp along the column which reduces the coupling back to the PLC. Any spectral amplitude and phase combination can be achieved by combining a tilt for amplitude and absolute offset for phase, limited only by the resolution of the system.

The insertion loss of the PSP is −14 dB. This high loss value is partially due to phase errors in the fabricated WGR, as well as an unoptimized transition from the guided region to free space. Both issues can be corrected in a subsequent run. We anticipate that system losses of ~7 dB can be achieved, limited by WGR coupling inefficiency and by losses of the 2D assembly. Thermal fluctuations in the system which may change slightly the position of the grid lines can be compensated with the written phase functions on the SLM and should not adversely affect the performance.

The PSP that we implemented supports one polarization only, due to our choice of grating and the LCoS SLM. Solutions providing support for both polarizations are discussed in Section 5.

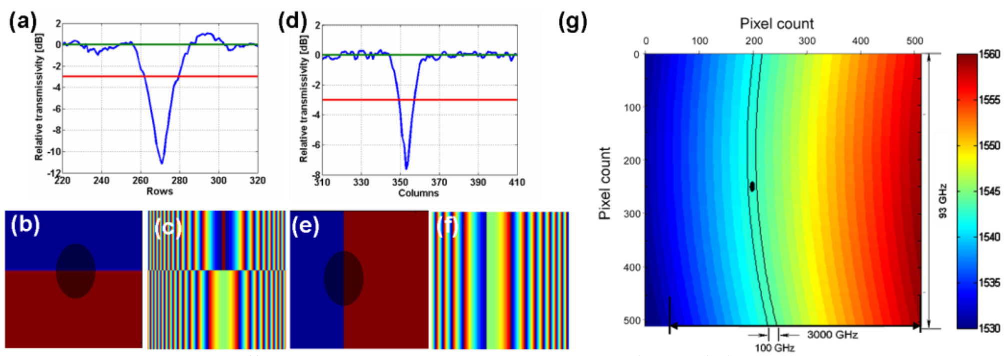

Fig. 3. Finding different wavelength positions with a 0-π step phase technique: (a-c) - Scanning the SLM with a phase step along the WGR direction results in the vertical position and size of the spot at specific wavelengths. The phase step is applied on top of the curved phase in order to reduce losses. The beam width (18 pixels) determines the spectral resolution of the system. (d-f) – The same procedure when the phase step is applied in the bulk grating direction. The result determines the size of each WDM channels on the SLM, where the green line mark 0 dB level. (g) Different wavelength locations on the SLM. The WGR provides high resolution on narrow FSR. The bulk grating separates the WGR diffraction orders. Individual channels are fully resolved on two-dimensional space. The black lines mark the borders of a specific WDM channel while the black ellipse denotes the spot size for a specific wavelength on this channel as it appears on the SLM.

#149409 - $15.00 USD Received 16 Jun 2011; revised 30 Jun 2011; accepted 30 Jun 2011; published 13 Jul 2011

4. PSP demonstrations

Numerous spectral manipulations can be envisaged with the two-dimensional PSP, owing to its fine resolution across all channels within the C-band. We demonstrate in the following WDM channel spectral amplitude manipulations, spectral phase manipulations, and in-band amplitude and phase spectral manipulations.

4.1 Channel amplitude control – WDM blocker

As a first demonstration, we used our PSP as a channel selector by blocking or transmitting complete columns (WDM channels). Figure 4 shows demonstrations of 15 randomly selected channels for attenuation. Channel selection is performed by applying a phase tilt to the rejected channel set. It should be noted that the linear phase tilt which serves as the attenuation mechanism can be prescribed either along the dispersion or along the beam height. Better attenuation performance was achieved with the former method, as the beam is wider in the fast dispersion direction.

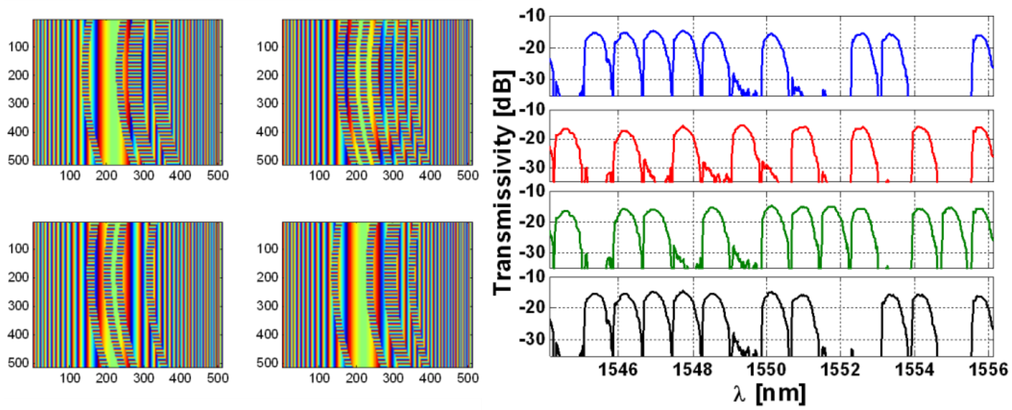

Fig. 4. Demonstration of channel selection with the 2D PSP. (Left) - The phase modulations as written on the SLM in the case of random selection of 15 WDM channels. Tilted phase was added on top of the curved equalization phase to attenuate channels. (Right) – Results of random selection of 15 WDM channels. A dynamic range of 20 dB is shown, limited by insufficient separation of WGR diffraction orders (or adjacent WDM channels).

4.2 Channel phase control –TODC and retimer

Two important applications of the PSP are tunable optical dispersion compensation (TODC) and channel retiming. To test the processor as a TODC, quadratic phase functions of varying radii were applied in the high dispersion direction to different channels (Fig. 5e), which result in different group delay slopes across each channel, hence chromatic dispersion (CD). An independent quadratic phase is applied to each selected. The quadratic phase maps to CD values according to:

$$CD \equiv \frac{2\pi c}{\lambda^2}\frac{d^2\phi(\omega)}{d\omega^2} = \frac{\lambda_0^2}{2\pi c_0}\frac{d^2\phi(x)}{dx^2}\left(\frac{dx}{d\lambda}\right)^2 = \frac{\lambda_0}{c_0}\frac{1}{R}\left(\frac{dx}{d\lambda}\right)^2 \tag{6}$$

where $\phi(x) = k_0 \cdot x^2/2R$ is the parabolic approximation to a curved phase, λ_0 is the wavelength in vacuum, c_0 is the speed of light, k_0 is the wave vector, $1/R$ is the applied curvature, $dx/d\lambda$ is the spatial dispersion and CD is the chromatic dispersion in units of ps/nm.

We performed group delay measurements with various curvature values applied to the channels (see Fig. 5(a) and 5(b)). As the slopes of the group delay are equivalent to CD, it can be seen that independent CD values can be applied to each channel. Our system is able to

#149409 - $15.00 USD Received 16 Jun 2011; revised 30 Jun 2011; accepted 30 Jun 2011; published 13 Jul 2011

compensate for CD values up to ± 750 ps/nm for each WDM channel. Larger CD values are achievable but will result in spectral narrowing [9] as shown in Fig. 6(a).

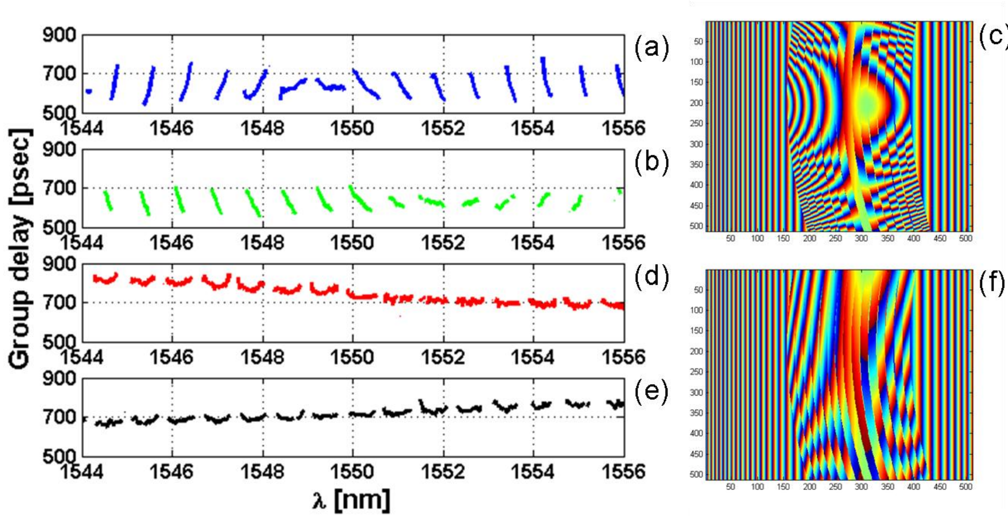

Fig. 5. Example of phase manipulation for 15 channels. (a-b) group delay slopes applied to each channel are equivalent to different CD compensation values. (c) The relevant phase pattern that was written on the SLM, consisting of varying quadratic phases. (d-e) Different group delay values applied to the selected 15 channels. (f) The relevant phase pattern that was written on the SLM, consisting of varying linear slopes.

A different phase manipulation is shown in Fig. 5(d) and 5(e). Channel retiming is achieved by applying linear phase along the spectrum, resulting in constant and controllable group delays per channel or channel retiming. Time offsets as large as ± 100 ps are demonstrated along 15 channels. The expression for the retiming is given by [20]:

$$\tau_{GD} \equiv \frac{d\phi(\omega)}{d\omega} = -\frac{d\phi(x)}{dx}\frac{dx}{d\lambda}\frac{d\lambda}{d\omega} = -\frac{\lambda_0}{c_0}\theta\left(\frac{dx}{d\lambda}\right) \tag{7}$$

where $\phi(x) = k_0 \cdot \theta \cdot \cdot x$ is the linear phase function applied along the channel, k_0 is the wave vector, and θ the phase slope angle in radians (under small angle approximation).

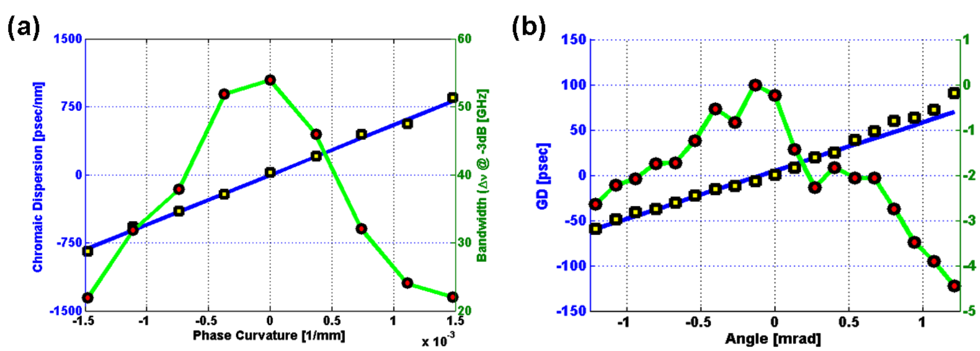

Fig. 6. The performance of the two-dimensional PSP when used as a TODC and as a retimer. (a) TODC performance: theoretical (Blue line) and measured (Yellow squares) CD values and bandwidth (Green) versus curvature. As the phase curvature values are larger, narrowing becomes dominant and the bandwidth is reduced down to 23 GHz FWHM for CD values of ± 750 ps/nm. (b) retimer performance: theoretical (Blue line) and measured (Yellow squares) GD values and loss (Green) versus slope angle measured in milliradians. As the phase slope becomes larger, the GD increases. However, large slopes results in high coupling losses.

#149409 - $15.00 USD Received 16 Jun 2011; revised 30 Jun 2011; accepted 30 Jun 2011; published 13 Jul 2011

Applying linear phase along the spectral channel results also in losses which become larger as the slope increases as shown in Fig. 6b. Those losses limit the amount of GD that can be achieved in the retiming mode. Thus, phase curvatures result in group delay slopes or CD values, while phase slopes result in constant group delays or retiming. TOCD range is primarily limited by spectral narrowing and retiming is limited by loss, both limitations arising from the coupling losses back to the output fiber through the PSP.

4.3 In-band channel manipulations – phase/amplitude carving

Since the spectral components of the communication C-band are dispersed along the two dimensional SLM, independent phase and amplitude spectral manipulations can be prescribed within each WDM channel.

Figure 7(a) demonstrates the use of the PSP for spectral carving by imparting unique attenuation features onto each WDM channel spectrum. This technique can be used to split the spectral channel into sub-bands or to attenuate spectral features and enhance the signal quality. Due to the high resolution of the PSP, almost any spectral shape can be prescribed for each channel, subject to the resolution constraint.

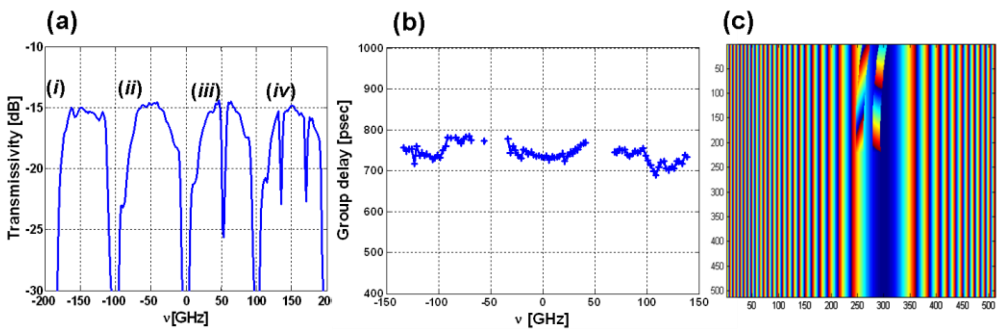

Fig. 7. Demonstration of inband manipulations: (a) spectral carving across the channel bandwidth for four contiguous WDM channels: (i) spectral flattening (ii) without modulation, (iii) spectrum carved to two sub-bands, (iv) spectrum carved to three sub-bands. (b) Example of half-channel group delay manipulation for 3 channels. A time split of 50 psec is obtained (c) The applied phase pattern on the SLM for the 3 half slopes case.

An interesting option which takes advantage of the high resolution of our PSP is to perform retiming of spectral components within a channel. Figure 7-(b) demonstrates such an example. A phase slope was applied on half of the three main channels. The result is a time delay that depends on the local slope along part of the channel [21-22]. For the left channel a positive slope was applied resulting in time delay for half of the channel, while for the right channel a negative slope was used resulting in a time advance for the half channel

5. Solutions for supporting dual polarizations

As mentioned previously, the current arrangement of our two-dimensional PSP operated for only a single polarization, due to the SLM and bulk grating.

There are two possible schemes in order to overcome this limitation which will result in a polarization-insensitive PSP. The first is by using components which are polarization insensitive. In this case one might substitute a MEMS based SLM [23] combined with a low-polarization dependent grating. An alternative approach is to design a system with polarization diversity as shown in Fig. 8.

In this solution, two PLC's are aligned together before the bulk grating. A polarization beam splitter and a polarization rotator are added to ensure that both polarizations are aligned after the WGR output. Since the angular dispersion of the two WGR is identical, the Fourier lens will project the spectral component onto the same position on the SLM, hence the same SLM can be used for applying phase and amplitude modulation to the various spectral components for both polarizations.

#149409 - $15.00 USD Received 16 Jun 2011; revised 30 Jun 2011; accepted 30 Jun 2011; published 13 Jul 2011

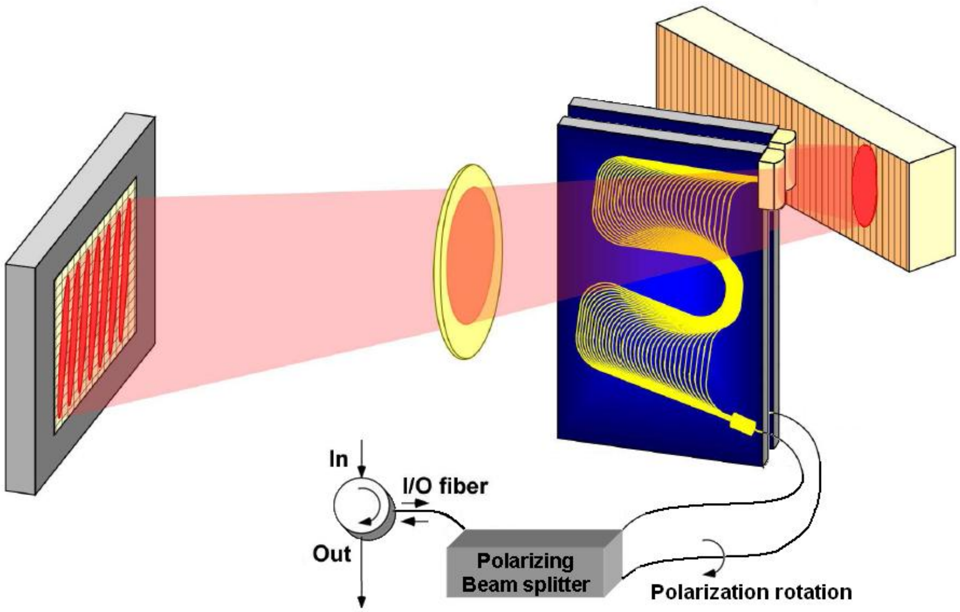

Fig. 8. Layout of a potential polarization insensitive PSP solution based on two PLC aligned together before the bulk grating. A polarizing beam splitter is used to separate the two incoming polarizations and a polarization rotator is added to ensure that both polarizations are aligned after the WGR output.

6. Summary

We demonstrated the functionality of our two-dimensional photonic spectral processor, which is capable of modulating a communication signal's spectral components in amplitude and phase. Our system's high resolution and full control along the entire C-band brings tremendous possibilities for wavelength manipulations useful in controlling and improving WDM signals in optical communication systems.

The two-dimensional PSP realized in our lab was assembled on an optical table using conventional optomechanical mounts. The arrangement would have to be compactly packaged for a more practical realization that can be deployed in the field. Such a realization would have to address the dual polarization support, as described in Section 5, as well as clever folding solutions such that the system's optical height is reduced. Currently the size of the WGR is the limiting factor in the vertical direction. A 90° rotating prism could be inserted in the optical system to orient the PLC in the horizontal direction, thereby achieving a slender optical system.